Shape-Induced Enhanced Luminescent Properties of Red Phosphors: $Sr_2MgSi_2O_7:Eu^{3+}$ Nanotubes

Junxi Wan,[a] Zhenghua Wang,[a] Xiangying Chen,[a] Li Mu,[a] and Yitai Qian*[a]

Keywords: Nanotubes / Silicates / Hydrothermal synthesis / Photoluminescence

$Sr_2MgSi_2O_7:Eu^{3+}$ nanotubes with red phosphor luminescent properties were successfully synthesized via a low-temperature hydrothermal route in order to understand the underlying relationship between shape and luminescent properties. The one-dimensional shape results in an obvious improvement of color purity. From emission spectra, the relative intensity of $^5D_0\rightarrow{}^7F_2$ to $^5D_0\rightarrow{}^7F_1$ transitions in tubular phosphors is higher than that of bulk material. The better color purity results from the more distorted lattices and relatively lower crystal symmetry around Eu^{3+} ions, which ascribes to the large surface area due to synthesize it in the form of nanotubes. Furthermore, the as-synthesized tubular red phosphor has shorter fluorescent lifetime and blue-shift phenomenon in excitation spectra than that of the bulk counterpart. Based on these results, shape-induced luminescent properties improvement is proposed as an efficient way to obtain red phosphors with high color purity.

Introduction

Since decades, phosphors doped with rare earth ions have attracted great interest.[1–4] Among those rare earth ions, the Eu^{3+} ion as a red luminescent activator in many host materials[5–10] has been studied intensively. Major emissions are centered at 590 nm ($^5D_0\rightarrow{}^7F_1$) and 616 nm ($^5D_0\rightarrow{}^7F_2$), corresponding well to orange and red color, respectively. So, the relative intensities of $^5D_0\rightarrow{}^7F_2$ to $^5D_0\rightarrow{}^7F_1$ transitions in phosphors are important for their applications. In order to obtain red phosphors with high color purity, it is necessary to increase the relative intensity of $^5D_0\rightarrow{}^7F_2$ to $^5D_0\rightarrow{}^7F_1$ transitions. It is well known that the relative intensities of the $^5D_0\rightarrow{}^7F_2$ to $^5D_0\rightarrow{}^7F_1$ transitions strongly depend on the local symmetry of Eu^{3+} ions.[11–13] The peak at 616 nm is due to the forced electric dipole transition ($^5D_0\rightarrow{}^7F_2$), which is allowed on condition that the europium ion occupies a site without an inverse center. Its intensity is hypersensitive to crystal environments. A relatively strong $^5D_0\rightarrow{}^7F_2$ transition is associated with a relatively low local symmetry of Eu^{3+} ions. The better color purity might result from the more distorted lattices and relatively lower crystal symmetry. Consequently, a change of the crystal structure of host materials can produce a good red phosphor.[14] However, shape and size are now regarded as particularly important factors influencing the chemical and physical properties of the materials.[11–13,15–21] If materials were fabricated in the form of a one-dimensional nanostructure, they would be expected to be highly functionalized materials as a result of both shape-specific and quantum confinement effects, acting as optically functional host materials. Based on this viewpoint, a possible way to improve the performance of current phosphors is to synthesize them in the form of 1D nanostructures. Nanotubes possess especially large surface area and high surface energy owing to their inner and outer surfaces, which could lead to a high degree of disorder and correspondent lower symmetry of crystal field around Eu^{3+} ions.[16,17] This lower symmetry of the crystal field will result in a higher relative intensity of $^5D_0\rightarrow{}^7F_2$ to $^5D_0\rightarrow{}^7F_1$ transitions. Therefore, it is favorable to get red phosphors with high color purity while the host materials are fabricated in the form of nanotubes. Only few efforts have been made to test and apply this idea and to develop new red phosphors.

We have synthesized a tubular Eu^{3+}-doped $Sr_2MgSi_2O_7$ red phosphor via a hydrothermal route. The as-synthesized phosphor has better color purity, which illustrates the validity and practicability of the idea that shape influences the improvement of luminescent properties. To our best knowledge, this is the first report about hydrothermal synthesis of Eu^{3+}-doped $Sr_2MgSi_2O_7$ nanotubes.

Results and Discussion

The phase purity and phase structure of as-prepared samples were characterized by the X-ray powder diffraction (XRD) patterns, using a Philips X′pert X-ray diffractometer equipped with graphite-monochromatized Cu-

[a] Hefei National Laboratory for Physical Sciences at Microscale and Department of Chemistry, University of Science and Technology of China,
Hefei, Anhui 230026, People's Republic of China
Fax: +86-551-3607402
E-mail: ytqian@ustc.edu.cn

Kα radiation (λ = 1.54178 Å). Samples for XRD analysis were prepared by dispersing the as-synthesized phosphors into absolute ethanol, then spreading several drops of this suspension on a clear silicon wafer, and then letting the solvent evaporate slowly at room temperature. The transmission electron microscopy (TEM) images and corresponding selected area electron diffraction (SAED) pattern were performed with a Hitachi H-800 transmission electron microscope using an accelerating voltage of 200 kV. Photoluminescence (PL) spectra and luminescent decay curve were recorded on a Fluorolog-3-TAU fluorescence spectrophotometer with an Hg lamp at room temperature.

Figure 1 shows the XRD patterns of as-synthesized Eu^{3+}-doped $Sr_2MgSi_2O_7$ red phosphors. All the diffraction peaks can readily be indexed to a pure tetragonal structured $Sr_2MgSi_2O_7$ with cell constants of a = 7.993 Å, and c = 5.158 Å, which are in good agreement with the values in the literate (JCPDS card No. 75–1736, a = 7.996 Å, and c = 5.152 Å). No obvious impurity phase can be detected. Compared to the XRD patterns of bulk phosphor (Figure 1, a) and as-synthesized sample (Figure 1, b), the intensity of the XRD peaks from as-synthesized sample is weaker than that of the bulk phosphor. Some weak peaks in Figure 1 (b) are nearly invisible. The intensification of peaks from bulk phosphor would result in improved luminescent intensity due to the increase of crystallinity. Table 1 shows representative comparisons of half-width and relative intensities of the XRD peaks from bulk and as-prepared sample. In Table 1, only the eight strongest peaks of both XRD patterns are listed. The differences of the eight strongest peaks of both XRD patterns are sufficient to demonstrate the fine-structural differences in the bulk and as-prepared phosphors. The differences of relative intensities of the XRD peaks indicate that the as-synthesized sample has a tendency to grow only in one direction. The increase of half-width of XRD peaks from as-prepared sample indicates the nanometer-scale sizes of sample. These differences in XRD peaks would lead to enhanced luminescent properties of phosphors. These results are further evidenced by the following TEM images and luminescent spectra.

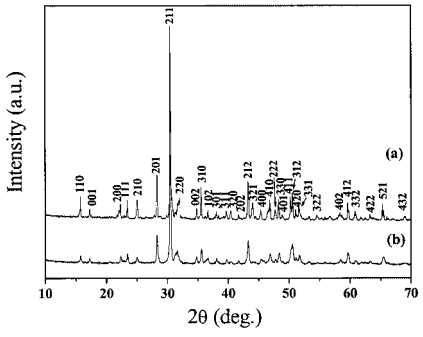

Figure 1. XRD patterns of the as-synthesized (a) bulk $Sr_2MgSi_2O_7$:Eu^{3+} and (b) $Sr_2MgSi_2O_7$:Eu^{3+} nanotubes.

TEM analysis has provided further insight into the microstructural details of these nanotubes. As shown in Figure 2, all samples dispersed on to the TEM copper grids have uniform nanotube morphologies with open ends. The as-synthesized nanotubes have diameters of about 15 nm and lengths up to several hundreds of nanometer. Figure 2 (b) shows two $Sr_2MgSi_2O_7$ nanotubes (the white arrows shown) parallel to the electron beam, from which the hollow structure features can be clearly seen with an inner diameter of about 10 nm and an outer diameter of about 20 nm. The electron diffraction patterns (inset in Figure 2, b), taken from bundles of $Sr_2MgSi_2O_7$ nanotubes, indicate that the nanotubes are crystalline. This result is in agreement with that of XRD pattern.

Table 1. Comparisons of eight strongest peaks in XRD patterns from bulk $Sr_2MgSi_2O_7$:Eu^{3+} and $Sr_2MgSi_2O_7$:Eu^{3+} nanotubes, respectively.

Indexing peaks	Bulk $Sr_2MgSi_2O_7$:Eu^{3+}		$Sr_2MgSi_2O_7$:Eu^{3+} nanotubes	
	Relative intensity	Half-width [mm]	Relative intensity	Half-width [mm]
110	12%	0.161		
201	23%	0.123	26%	0.191
211	100%	0.120	100%	0.196
310	17%	0.121	14%	0.286
212	20%	0.020	22%	0.260
330	10%	0.135	11%	0.297
411	11%	0.129	14%	0.279
312	13%	0.125	18%	0.271
412			12%	0.201

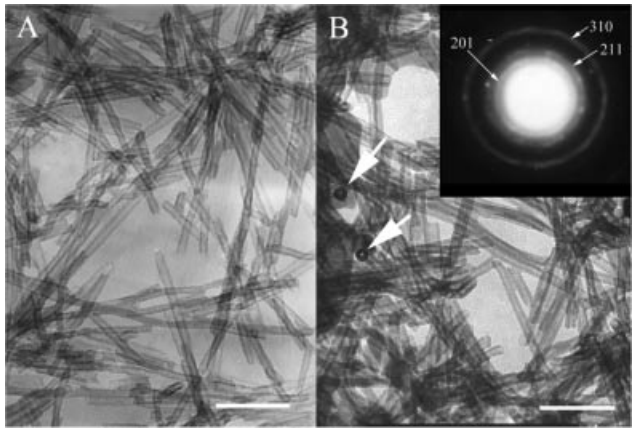

Figure 2. Representative TEM images and SAED pattern of synthesized samples; length of bar: 100 nm.

The excitation spectra of Eu^{3+}-doped $Sr_2MgSi_2O_7$ nanotubes and bulk phosphor for the emission at 616 nm are shown in Figure 3. The broad band on the excitation spectra is excitation from the ground state of the 4f shell to an Eu–O charge transfer state.[22] Moreover, the CTS (charge transfer state absorption) peak position of $Sr_2MgSi_2O_7$ nanotubes shows a blue-shift phenomenon compared with the bulk counterpart. The CTS peaks of the nanotubes and bulk phosphor center at 250 nm and 261 nm, respectively. A similar observation was reported in nanometer Y_2O_3:Eu phosphor.[19] The sharp absorption peaks on excitation

spectra is a characteristic of rare earth ions as a result of transitions within the 4f shell, which is shielded from environmental effects by the outer shell electrons.[23] Thus, these peaks position are consistent.

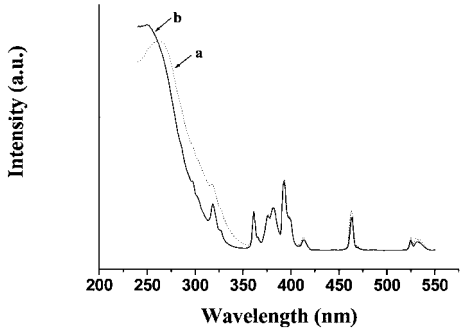

Figure 3. Excitation spectra of (a) bulk $Sr_2MgSi_2O_7$:Eu^{3+} phosphor, (b) $Sr_2MgSi_2O_7$:Eu^{3+} nanotubes.

Figure 4 shows the emission spectra of as-synthesized Eu^{3+}-doped $Sr_2MgSi_2O_7$ nanotubes and bulk phosphor. Both of them consist of two main peaks centered at 590 nm and 616 nm, which come from the transitions of $^5D_0 \rightarrow {}^7F_1$ and $^5D_0 \rightarrow {}^7F_2$, respectively. The most intense emission is the $^5D_0 \rightarrow {}^7F_2$ transition located in 616 nm, corresponding to the red emission, in good accordance with the Judd–Ofelt theory.[24] Compared with the bulk phosphor, the luminescent properties of as-synthesized $Sr_2MgSi_2O_7$ nanotubes are obviously enhanced. The emission intensity of the $^5D_0 \rightarrow {}^7F_2$ transition is 3.2 times that of the $^5D_0 \rightarrow {}^7F_1$ transition. However, the ratio only is 1.7 for bulk phosphor. Only the emission peak located at 616 nm of $Sr_2MgSi_2O_7$ nanotubes has a remarkable enhancement than that of bulk phosphor. This phenomenon indicates that more Eu^{3+} occupy sites with relatively low local symmetry. These results prove the idea that red phosphors with high color purity can be obtained by changing the shape of host materials.

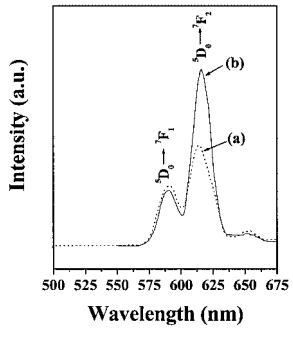

Figure 4. Emission spectra of (a) bulk $Sr_2MgSi_2O_7$:Eu^{3+} phosphor, (b) $Sr_2MgSi_2O_7$:Eu^{3+} nanotubes.

The decay time of Eu^{3+} fluorescence of Eu^{3+}-doped $Sr_2MgSi_2O_7$ nanotubes and bulk phosphor were measured at room temperature. Figure 5 shows the results that the lifetime values are 1.2 ms of $Sr_2MgSi_2O_7$ nanotubes and 2.3 ms of bulk phosphor, respectively. Similar phenomena was observed in nanometer ZnS:Mn^{2+}[25] and Y_2O_3:Eu^{3+} phosphors.[26] The shorter lifetime value can be attributed to the fact that the $Sr_2MgSi_2O_7$ nanotubes have relatively more defects, which results from the increase of the surface/volume ratio in the nanotubes. The shorter decay time is beneficial to PDP (plasma display panel) applications. With further optimization, Eu^{3+}-doped $Sr_2ZnSi_2O_7$ may serve as good red phosphor candidates. Further research is underway.

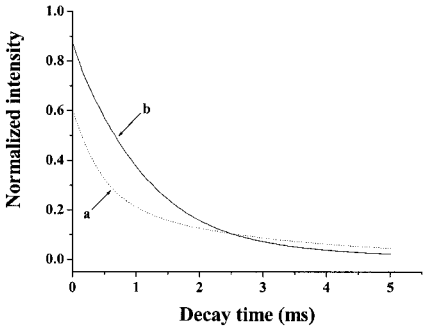

Figure 5. Normalized decay curve of (a) bulk $Sr_2MgSi_2O_7$:Eu^{3+} phosphor, (b) $Sr_2MgSi_2O_7$:Eu^{3+} nanotubes.

Conclusions

In summary, we have successfully synthesized pure tetragonal phased $Sr_2MgSi_2O_7$:Eu^{3+} nanotubes via a low-temperature hydrothermal route at 200 °C for 2 days. The resulting tubular red phosphor has a shorter decay time than that of the bulk counterpart. A close study of the excitation spectra points to a blue-shift phenomenon for the $Sr_2MgSi_2O_7$:Eu^{3+} nanotubes. The emission spectra show that the as-prepared tubular red phosphor has a better color purity than the bulk counterpart. The improvement of luminescent properties was analyzed and the influence of shape on luminescence was explored. Based on these results, shape-induced luminescent properties improvement is a simple and efficient way to obtain red phosphors with high color purity. This idea provides helpful guidance for the application of the $Sr_2MgSi_2O_7$:Eu^{3+} red phosphor. Furthermore, this strategy may also be applied to other rare earth ion-doped phosphors.

Experimental Section

All reagents were purchased from Shanghai Chemical Reagent Co. and used without further purification. Distilled water and absolute ethanol, degassed with N_2 for one hour, were used. In a typical procedure, 2 mmol of $Sr(NO_3)_2$, 1 mmol of $Mg(NO_3)_2 \cdot 6H_2O$, and 0.1 mmol of $EuCl_3$ were dissolved in a mixture of 5 mL of distilled water and 30 mL of absolute ethanol whilst stirring in a Teflon liner of 60 mL capacity. Then an aqueous solution of 2 mmol of $Na_2SiO_3 \cdot 9H_2O$ dissolved in 5 mL of distilled water was slowly added. After about 10 minutes, the aqueous solution of 1 g of NaOH dissolved in 5 mL of distilled water and 2 mL of 85% $N_2H_4 \cdot H_2O$ were added whilst stirring. Hydrazine hydrate was used to prevent reduction of Eu^{3+}. Finally, the mixture was degassed with N_2 for another one hour. Then, the liner was sealed in a stainless steel autoclave, first aged at 90 °C for 12 h, and then maintained at 220 °C for 2 days. After cooled to room temperature naturally,

the resulting white solid products were filtered off, washed with distilled water and absolute ethanol for several times, respectively, and finally calcined in air at 800 °C for 6 h. For comparison, Eu^{3+}-doped $Sr_2MgSi_2O_7$ red phosphor was also prepared via solid-state reaction at 1300 °C for 3 h in air according to the literature.[27] The as-synthesized sample was finely ground to give a powder that was used for further characterization.

Acknowledgments

This work was supported by the National Natural Science Foundation of China and the 973 Project of China.

[1] G. Wakefield, E. Holland, P. J. Dobson, J. L. Hutchison, *Adv. Mater.* **2001**, *13*, 1557–1560.
[2] H. Lin, E. Y. B. Pun, X. J. Wang, X. R. Liu, *J. Alloys Compd.* **2005**, *390*, 197–201.
[3] A. N. Georgobiani, A. N. Gruzintsev, C. Barthou, P. Benalloul, *Inorg. Mater.* **2004**, *40*, 840–844.
[4] Y. Liu, C. N. Xu, *Appl. Phys. Lett.* **2004**, *84*, 5016–5018.
[5] Q. L. Liu, Y. Bando, F. F. Xu, C. C. Tang, *Appl. Phys. Lett.* **2004**, *85*, 4890–4892.
[6] O. Lehmann, K. Kompe, M. Haase, *J. Am. Chem. Soc.* **2004**, *126*, 14935–14942.
[7] Y. Zhang, Y. D. Li, *J. Alloys Compd.* **2004**, *370*, 99–103.
[8] S. S. Yi, J. S. Bae, B. K. Moon, J. H. Jeong, J. H. Kim, *Appl. Phys. Lett.* **2005**, *86*, 071921.
[9] A. Huignard, V. Buissette, A. C. Franville, T. Gacoin, J. P. Boilot, *J. Phys. Chem. B* **2003**, *107*, 6754–6759.
[10] J. H. Kang, W. B. Im, D. C. Lee, J. Y. Kim, D. Y. Jeon, Y. C. Kang, K. Y. Jung, *Solid State Commun.* **2005**, *133*, 651–656.
[11] Z. G. Wei, L. D. Sun, C. S. Liao, J. L. Yin, X. C. Jiang, C. H. Yan, *J. Phys. Chem. B* **2002**, *106*, 10610–10617.
[12] Z. G. Wei, L. D. Sun, C. S. Liao, X. C. Jiang, C. H. Yan, *J. Appl. Phys.* **2003**, *93*, 9783–9788.
[13] Z. G. Wei, L. D. Sun, X. C. Jiang, C. S. Liao, C. H. Yan, Y. Tao, J. Zhang, T. D. Hu, Y. N. Xie, *Chem. Mater.* **2003**, *15*, 3011–3017.
[14] C. J. Jia, L. D. Sun, F. Luo, X. C. Jiang, L. H. Wei, C. H. Yan, *Appl. Phys. Lett.* **2004**, *84*, 5305–5307.
[15] X. C. Jiang, L. D. Sun, C. H. Yan, *J. Phys. Chem. B* **2004**, *108*, 3387–3390.
[16] G. S. Wu, Y. Lin, X. Y. Yuan, T. Xie, B. C. Cheng, L. D. Zhang, *Nanotechnology* **2004**, *15*, 568–571.
[17] C. F. Wu, W. P. Qin, G. S. Qin, D. Zhan, J. S. Zhang, S. H. Huang, S. Z. Lu, H. Q. Liu, H. Y. Lin, *Appl. Phys. Lett.* **2003**, *82*, 520–522.
[18] Y. He, Y. Tian, Y. F. Zhu, *Chem. Lett.* **2003**, *32*, 862–863.
[19] T. Igarashi, M. Ihara, T. Kusunoki, K. Ohno, T. Isobe, M. Senna, *Appl. Phys. Lett.* **2000**, *76*, 1549–1551.
[20] D. K. Williams, H. Yuan, B. M. Tissue, *J. Lumin.* **1999**, *83–84*, 297–300.
[21] G. Wang, Z. D. Wang, Y. X. Zhang, G. T. Fei, L. D. Zhang, *Nanotechnology* **2004**, *15*, 1307–1311.
[22] M. Yin, W. Zhang, S. Xia, J.-C. Krupa, *J. Lumin.* **1996**, *68*, 335–339.
[23] G. Blasse, *Handbook on the Physics and Chemistry of Rare Earths*, vol. 4, North Holland, Amsterdam, **1976**.
[24] B. R. Judd, *Phys. Rev.* **1962**, *127*, 750–761.
[25] R. N. Bhargava, D. Gallagher, X. Hong, A. Nurmikko, *Phys. Rev. Lett.* **1994**, *72*, 416–419.
[26] W. W. Zhang, W. P. Zhang, P. B. Xie, M. Yin, H. T. Chen, L. Jing, Y. S. Zhang, L. R. Lou, S. D. Xia, *J. Colloid Interface Sci.* **2003**, *262*, 588–593.
[27] Y. H. Lin, C. W. Nan, X. S. Zhou, J. B. Wu, H. F. Wang, D. P. Chen, S. M. Xu, *Mater. Chem. Phys.* **2003**, *82*, 860–863.

Received: June 4, 2005
Published Online: September 12, 2005

